Carbohydrate Polymers 117 (2015) 710–721

Contents lists available at ScienceDirect

Carbohydrate Polymers

journal homepage: www.elsevier.com/locate/carbpol

Solid state NMR and IR characterization of wood polymer structure in relation to tree provenance

Ilaria Santoni[a], Emanuela Callone[b], Anna Sandak[a], Jakub Sandak[a,*], Sandra Dirè[b]

[a] Trees and Timber Institute IVALSA/CNR, via Biasi 75, 38010 San Michele All'Adige, Italy
[b] Industrial Engineering Department, University of Trento, v. Mesiano 77, 38123 Trento, Italy

ARTICLE INFO

Article history:
Received 6 November 2013
Received in revised form
15 September 2014
Accepted 19 October 2014
Available online 30 October 2014

Keywords:
Solid state NMR spectroscopy
Mid-infrared spectroscopy
Wood provenance
PCA

ABSTRACT

^{13}C nuclear magnetic resonance and mid-infrared spectroscopies were used for characterizing changes in the chemical structure of wood polymers (cellulose, hemicellulose and lignin) in relation to the tree growth location. Samples of three provenances in Europe (Finland, Poland and Italy) were selected for studies. The requirement was to use untreated solid wood samples to minimize any manipulation to the nanostructure of native wood.

The results confirm that the chemical and physical properties of samples belonging to the same wood species (*Picea abies* Karst.) differ due to the origin. Both FT-IR and dynamic NMR spectroscopies were able to correctly discriminate samples originating from three different provenances in Europe. Such methods might be very useful for both, research and understanding of wood microstructure and its variability due to the growth conditions.

1. Introduction

The adaptation of species had been scientifically demonstrated by Darwin (1868). Local climate, soil, slope, forest density, silvicultural practices, fungi, wildlife, disease and other factors can strongly influence the tree growth and consequently, wood formation. The timber in a given site carries a record of all the conditions listed above. As an adaptation mechanism of trees to different site conditions several variations in the tree-ring structure have been observed by Miina (2000), Park and Spicker (2005), Manetti and Cutini (2006) and Andreassen, Solberg, Tveito, and Lystad (2006) among others. Norway spruce (*Picea abies* Karst.), often called whitewood, is a northern and central European species, living primarily in the mountainous areas. The vertical limit for the spruce presence in the Alps is at an altitude of ~2200 m. There are three main regions of spruce presence in Europe:

- Scandinavia, West Siberia (up to the Urals), Belarus and Northeast Poland.
- Mountainous areas of Central Europe—the Sudetes and the Carpathian Mountains.
- Southern Europe including the Balkans and the Alps.

According to recent forest inventories, the actual distribution of spruce is much wider than its natural ranging (Spicker, 2000).

The Norway spruce wood from northern provenances (Scandinavian countries) has the highest overall density and percentage of latewood comparing to trees growing in Central and Southern Europe (Skrøppa, Hylen, & Dietrichson, 1999). Krzysik (1978) reported that different amounts of cellulose, hemicelluloses, lignin, and extractive components were measured in spruce wood from different provenances. Analogous observations were noticed for other wood species; *Eucalyptus globulus* (Miranda & Pereira, 2002), *Pinus helepensis* (Tahar, Tayeb, & Chaabane, 2007), *Pinus ponderosa* (Smith, Peloquin, & Passoff, 1969). It is expected, therefore, that trees growing in various parts of the world would differ in such a way to discriminate their specific distinctive features.

The currently employed PEFC (Programme for the Endorsement of Forest Certification), used for tracking the wood flow from the forest to the mill system, is based only on written documentation. Several methods including chemical and genetic fingerprinting are currently employed for verification of product identity by examining its chemical or genetic composition (Dykstra et al., 2002). Chemical fingerprinting methods include: analysis of trace elements, pyrolysis, gas chromatography, as well as, near- and

* Corresponding author. Tel.: +39 0461660232; fax: +39 0461650045.
E-mail addresses: santoni@ivalsa.cnr.it (I. Santoni), callonee@ing.unitn.it (E. Callone), anna.sandak@ivalsa.cnr.it (A. Sandak), sandak@ivalsa.cnr.it (J. Sandak), sandra.dire@ing.unitn.it (S. Dirè).

http://dx.doi.org/10.1016/j.carbpol.2014.10.057
0144-8617/

mid- infrared spectroscopies. Genetic fingerprinting methods consist of DNA marker analysis from one or more of the following genomes: nuclear, plastid or mitochondrial. Even if several successful applications of the above techniques have already been reported, (Nielsen & Kjær, 2008; Sandak, Sandak, & Negri, 2010; Sandak, Sandak, & Negri, 2011; Sandak, Sandak, Cantini & Autino, 2014) none of these methodologies has reached a stage of development that would warrant its general use up to this point. Some techniques are too costly and/or time consuming for routinely use in timber tracking. These applications are limited to a small number of samples, to be investigated in the laboratory. On the contrary, infrared spectroscopy, as fast and non-destructive method, has been already applied for provenance certification and integral quality control of various food products (Burns & Ciurczak, 2008). Moreover, Rana, Müller, Naumann, and Polle (2008) used mid infrared spectroscopy for classification of European beech wood (*Fagus silvatica* L.) growing in various parts of Germany. The method properly classified wood regarding provenance in almost all investigated cases. Unfortunately, the detailed interpretation of infrared spectra and the following correlation of acquired data in order to discriminate the provenance are still questionable. Therefore, an additional research supporting better understanding of the infrared relation with wood provenance is of great interest.

Nuclear magnetic resonance (NMR) is becoming a routine technique in agro-food fields for quality control and traceability of cheese and wine (Sacchi & Paolillo, 2007; Aghemo, Albertino, & Gobetto, 2011; Mazzei & Piccolo, 2012; Ritota et al., 2012a; Ritota, Casciani, Failla, & Valentini, 2012b). It is expected, therefore, that it might have also a great potential in the field of wood traceability. The feasibility of this approach should be exploited, taking into account the wide use of NMR for studying chemical structure of wood (Gil & Neto, 1999; Maunu, 2002; Bardet et al., 2009; Mburu, Dumarcay, Huber, Petrissans, & Gerardin, 2007). Thus, many papers focus on the structural differences between natural and treated wood-based materials, the efficiency of chemical extraction methodologies, and characterization of its polymeric components. NMR characterization of wood was a subject in the archeological research to test the wood aging and storage effects of historical materials (Bardet, Foray, & Tran, 2002; Bardet, Foray, Maron, Goncalves, & Tran, 2004; Crestini, El Hadidi, & Palleschi, 2009). It has also been used for monitoring the decomposition level of forested areas (Preston, Trofymow, Niu, & Fyfe, 1998). Wood is, in its nature, a complex and heterogeneous material, considered as a matrix of three main polymers: cellulose, hemicellulose and lignin. The advantage of NMR technique is, therefore, in its ability to analyze a mixture of such polymers without extensive chemical modifications to obtain separated fractions. Several authors have reported NMR research results on lignin structures (Nimz, Robert, Faix, & Nemr, 1981; Malkavaara, Alén, & Kolehmainen, 2000; Capanema, Balakshin, & Kadla, 2004). Other studies have been dedicated to woody carbohydrates, hemicelluloses (Gil & Neto, 1999; Maunu, 2002) and cellulose (Newman, 1999; Larsson, Hult, Wickholm, Pettersson, & Iversen, 1999; Mansfield & Meder, 2003; Okushita, Komatsu, Chikayama, & Kikuchi, 2012). These have been a starting point for the following research on wood by solid state NMR. This has dealt with the structural modifications induced directly by processes such as pyrolysis, densification, bleaching, pulping or biodegradation (Sivonen, Maunu, Sundholm, Jamsa, & Viitaniemi 2002; Alesiani et al., 2005; Delmotte, Ganne-Chédeville, Leban, Pizzi, & Pichelin, 2008; Popescu, Larsson, & Vasile, 2011). Most of these works dealt with the ^{13}C cross polarization magic angle spinning (CPMAS) NMR technique, due to the high signal-to-noise ratio obtainable in a relatively short experimental time, despite the loss of quantitative reliability. However, it must be noted here that physical manipulation of wood, such as scratching and grinding while preparing suitable samples lead to changes in its polymeric structure, i.e. the composition appears to be method dependent to some extent (Viel, Capitani, Proietti, Ziarelli, & Segre, 2004; Bardet et al., 2002). This means that the results of liquid and solid state NMR analyses of isolated components are not comparable and, therefore, provide little information on the original structure of solid wood.

To get a fingerprint of the pristine material, two solutions have been proposed: the use of milled grains that unfortunately leads to the loss of resolution due to surface effects (Alesiani et al., 2005), and the employ of small cylindrical samples (Preston et al., 1998, Bardet et al., 2009). However, the preparation process of such samples is rather complicated and it is not possible to use high spinning rates, due to instability problems (Alesiani et al., 2005). Therefore, an alternative procedure should assure a proper representation of the complex wood structure while minimizing any chemo-physical manipulation of the wood during sample preparation.

Taking into account the above considerations, the aim of this research was to develop an original MAS NMR-based methodology (including experimental set-up and wooden sample preparation) for studies of chemical/physical wood properties. The overall objective was to characterize cellulose, hemicellulose and lignin of selected wood samples possessing intra-species differences resulting from variation of geographical provenance. Both IR and NMR spectroscopies, assisted by modern multivariate analysis, were investigated.

2. Material and methods

2.1. Material selection

Sets of Norway spruce (*P. abies* L. Karst.) wood samples collected in three different locations within Europe were used as experimental materials. The countries of origin included Finland, Poland and Italy, all differencing in geographical position, elevation, climate and silviculture. The summary of site characteristics is presented in Table 1. The procedure of samples harvesting, conditioning and preparation was described previously (Sandak et al., 2011). A small block (~20 mm width) was cut out from each undercut slab, assuring the opening of the radial plane. The samples were firstly dried (50 °C) and carefully conditioned to guarantee constant moisture content (~12% MC), minimizing the differences in the water signal measured by the spectroscopy. Because it was impossible to collect trees of exactly the same age, experimental samples were obtained from the adult wood zones assuring equal cambial age of the all investigated samples.

2.2. Chemical composition

The chemical content of main woody polymers was determined on milled samples from each provenance.

The concentration of cellulose was determined according to the Seifert procedure (by using acetylacetone–dioxane–hydrochloric acid) (Browning, 1967). Holocellulose content was obtained by wood delignification with sodium chlorite with the addition of acetic acid (Browning, 1967). The content of hemicellulose was computed as the difference between holocellulose and cellulose. The quantities of other wood components were determined according to the following standards: lignin (TAPPI T 222 om-06, 2006), hot water extractives (TAPPI T 207 cm-08, 2008), 1% NaOH extractives (TAPPI T 212 om-07, 2007b), organic solvent (ethanol) extractives (modified TAPPI T 204 cm-07, 2007a), ash content (TAPPI T 211 om-07, 2007c). The chemical analyses were repeated three times and maximum standard deviation of results was considered as a measurement error indicator.

Table 1
General characteristics of the provenance sites.

Country of origin	Country code	Elevation (m.a.s.l.)	Geographical coordinates		Climatic condition		Silvicultural details
			Latitude (N)	Longitude (E)	Mean annual T (°C)	Mean annual precipitation (mm)	
Italy	I	1700–1800	46°11′	11°50′	+2.4	1260	Natural stand
Finland	F	140	63°22′	30°42′	+2	650	Artificial forest
Poland	P	600–810	50°44′	16°9′	+8.4	600	Zone of industrial emissions

2.3. FT-IR-ATR analysis

The set of 30 samples (10 for each provenance) were analyzed by means of mid infrared spectroscopy using FT-IR spectrometer (ALPHA produced by Bruker Optics GmBH) equipped with a ZnSe external module for attenuated total reflection (ATR) with the following settings: 24 scans per sample; spectral resolution: 4 cm^{-1}, wavenumber range: 4000 to 600 cm^{-1}. The OPUS 7.0 (by Bruker Optics) software package was used for instrument control and data processing. An original procedure for selection of the representative samples was established on the base of samples homogeneity. First, an average spectrum representing one provenance was calculated from the set of all spectra acquired within samples of same provenance. Three samples with spectra closest (in term of spectral distance) to the average value were selected for NMR analysis. The homogeneity was quantified on the base of cluster analysis. The selection was essential to diminish the natural variability of woody material and to assure a compromise between the generality of results and the relatively time consuming NMR analyses.

2.4. NMR analysis

The nuclear magnetic resonance measurements were restricted to the nine representative samples (P1–P3, I1–I3, F1–F3) selected from the set of 30 samples measured by FT-IR. MAS NMR analyses were carried out with a Bruker 300WB (Bruker Biospin, Reihnstetten, DE) instrument operating at a proton frequency of 300.13 MHz. NMR spectra were acquired with a cross-polarization (CP) pulse sequence under the following conditions: ^{13}C frequency 100.07 MHz, $\pi/2$ pulse length 3.5 μs, ^{1}H decoupling pulse power 47 kHz, recycle delay 3 s, contact time range 0.2–9 ms, 2k scans, spectrum size 16k, time domain 1k with a line broadening of 30 Hz and no zero filling.

Samples in the form of rolled thin wood slices (thickness of ~100 μm) were packed in 4 mm diameter zirconia rotors, which were spun at 8 kHz under air flow. Both the sample shape and size ensure the use of a representative sample. The thickness and size of every wood slice were controlled, and both wood and HDPE sheets were weighted with an analytical balance KERN ABS220-4 (0.1 mg accuracy) in order to obtain comparable samples. The average weight of wood was 35.7 ± 2.0 mg. Rolled thin films could avoid both the instability problems of bulk cylinders under high spinning speed, which is necessary to eliminate the contribution of spinning sidebands, and the loss of resolution of milled grains due to surface effects (Alesiani et al., 2005).

In addition, the use of an internal standard was evaluated in order to ensure quantitative analysis and to estimate the measurement stability. For this purpose, a high-density polyethylene (HDPE) film, with a mass of ~6.5% the corresponding wood weight (average weight of HDPE film was 2.3 ± 0.1 mg), was rolled together with the wooden slice. The HDPE did not affect the NMR spectrum; its peak does not overlap with the wood signals. Bruker Topspin 1.3 software was used for data analysis and spectra deconvolution.

Basic CPMAS experiments were recorded to identify the main signals assigned to the wood and the HDPE. Since intrinsic parameters, like conformation and mobility depend both on homonuclear and heteronuclear interactions, variable contact time experiments (VCT) were performed in order to obtain complementary information. The CP spectrum intensity depends on two competing factors, the magnetization transfer by dipolar coupling and the spin–lattice relaxation times in the rotating frame. Thus, measuring spectrum intensity (M) as a function of CP contact time (t), it is possible to extract cross-relaxation parameters T_{CH} (cross-polarization rate constant) and $T_{1\rho(H)}$ (spin–lattice relaxation time) (Eq. (1)). Numerical estimation of T_{CH} and $T_{1\rho(H)}$ values are usually obtained by fitting the obtained experimental curve with single or multiple exponential laws according to homogeneity, segregation and/or domain size (Kolodziejski & Klinowski, 2002).

$$M(t) = M_0 \times e^{-t/T_{1\rho(H)}} \times (1 - e^{-t/T_{CH}}) \quad (1)$$

where $M(t)$ is the peak intensity as a function of contact time t, M_0 is the normalization constant, $T_{1\rho(H)}$ is the proton spin–lattice relaxation time in the rotating frame, and T_{CH} is the cross-polarization time constant.

2.5. Multivariate data analysis

Principal component analysis (PCA) and cluster analysis (CA) were used for evaluation of spectral data obtained by FT-IR and NMR spectroscopies. Mid infrared spectra were post-processed and evaluated with OPUS 7.0 software (Bruker Optics GmBH). Ward's algorithm and the calculation of Euclidean distances was applied when creating dendrograms of the CA. Identity test (part of the Opus package) was used for development of the PCA models discriminating woods due to the provenance. Unscrambler 10.2 (Camo Software) was used for PCA analysis of NMR data.

3. Results and discussions

The chemical composition of Norway spruce samples representing three different provenances is presented in Table 2. The apparent difference between quantities of cellulose and holocellulose within samples of all locations are negligible and smaller than the measurement error. It was confirmed by means of analysis of variance (ANOVA F-test) where not statistical difference between means was noticed. It was not possible, therefore, to explain (by wet chemistry analysis) the possible qualitative differences between carbohydrates extracted from woods of different origin. Some more evident differentiation due to provenance was, however, noticeable for the lignin, ash and extractives content as also confirmed with ANOVA (bolded numbers of F-values > F-critical in Table 2).

Selected physical properties, as summarized in Table 3, indicate clear morphological differentiation of spruce samples from Finland, Poland and Italy. The specific density and the late wood ratio of Italian wood samples were the lowest. The highest ring width was noticed for wood from Poland. The tendency followed the results of Franceschini et al. (2010) where the ring width is negatively correlated with the tree age. The yearly ring size was comparable for samples from Finland and Italy, even if the geographical locations were the most distant. However, the climatic conditions, especially the average yearly temperature and the length of vegetation season, were similar in both Finland and Italy.

Table 2
Mean contents of chemical components extracted from Norway spruce samples of different provenances.

Country code	Cellulose % (±1.36)	Lignin % (±0.25)	Holocellulose % (±1.80)	Hemicellulose % (±1.50)	Extractives % (±0.32)	Hot water soluble % (±0.30)	1% NaOH soluble % (±0.60)	Ash % (±0.26)
I	45.5	28.8	70.4	24.9	1.15	0.87	10.65	0.31
F	45.2	28.4	70.2	25	1.82	2.05	11.48	0.26
P	45.7	29.3	70.2	24.5	1.84	0.56	9.73	0.30
F-value	0.9	**14.9**	0.2	–	**26.1**	1.6	**13.6**	**6.2**

F-critical = 5.1.

Table 3
Physical characteristic of spruce samples.

Sample code	Density (g/cm^3)	Late wood ratio (mm/mm)	Age of tree (yr)	Average ring width (mm)
I1	0.42	0.27	127	1.08
I2	0.43	0.30	137	0.97
I3	0.39	0.17	131	1.60
F1	0.50	0.36	147	0.95
F2	0.56	0.38	141	1.14
F3	0.51	0.36	144	0.91
P1	0.46	0.30	100	1.59
P2	0.47	0.20	83	2.86
P3	0.45	0.28	99	1.80
F-value	17.5	5.1	48.7	5.0

F-critical = 5.1.

Fig. 1 presents results of FT-IR principal components analysis (PCA) performed on spectra collected from wood samples of three different provenances. A clear separation between groups was achieved after plotting the three first PC scores on the graph. These results for mid-IR are in correspondence with previous studies using near-IR. They proved that wood of the same species (*P. abies* Karst.) from different provenance can be separated through FT-NIR spectroscopy (Sandak et al., 2011). The question rises here: what are the chemical/physical bases for such distinction of different spruce woods?

The growing environment (including climate, soil, silviculture and the yearly variation of sun/rain), beside of genetic factors, strongly affects wood physiology, xylogenesis, tree morphology and, in consequence, wood chemical composition. The three structural polymers (cellulose, hemicelluloses and lignin) have an extremely complex cross-configuration and make up 90–98% of the woody matter. The chemical structure of cellulose, hemicelluloses and lignin is schematically presented in Fig. 2.

Cellulose is a linear homopolymer composed of β-D-glucopyranose units with high tendency to form hydrogen bonds. Chains of cellulose are organized together in microfibril structure where crystalline regions are alternate to amorphous ones. Microfibrils are then aggregated into fibrils which in turn are aggregated into cellulose fibers (Sjöström, 1981). The quantity and quality of cellulose varies between wood species and depends on the tree growing conditions.

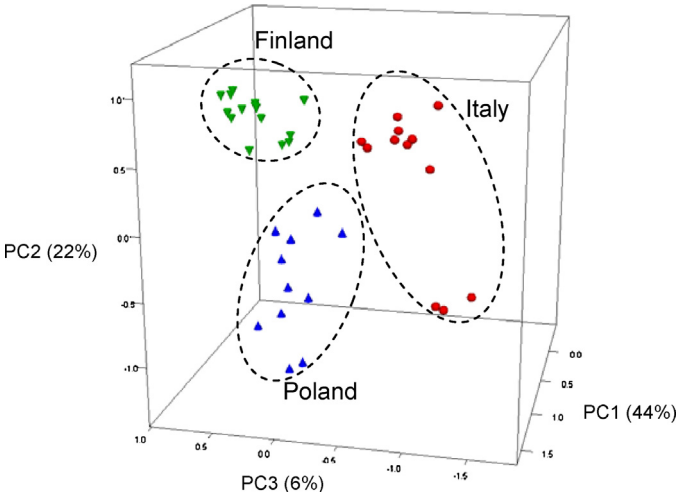

Fig. 1. FT-IR-based discrimination of the spruce woods due to provenance.

The chemical structure of lignin is very complex. Up to now, the detailed description of its composition and constitution is a matter of argue and scientific debate. The primary units are known, lignin is composed of phenylpropanoid units cross linked in non-regular and amorphous structures. The lignin composition in soft- and hard-woods is different. The softwoods lignin is a polymer consisting mostly of guaiacyl units with only small amount of *p*-hydroxyphenyl and syringyl units. The hardwood lignin is composed of syringyl and guaiacyl units with small amount of *p*-hydroxyphenyl units (Fengel & Wegener, 1989).

Hemicelluloses are another structural polymers composed of monomeric components, where most significant are arabinose, xylose and galactose, mannose and methylglucuronic acid. Hemicelluloses are chemically connected to both lignin and cellulose. Hemicelluloses and lignin are considered as the encrusting material between cellulose microfibrils.

Multivariate analysis, including principal component analysis (PCA) are most versatile chemometric methods to be applied for complex materials such as wood. Series of dedicated studies were performed for development of statistical models differentiating wood due to provenance. Results of PCA applied to IR spectra of wood samples investigated are presented in Fig. 1. The model has been developed with Identity test (software module within OPUS package) by pre-processing spectra with the second derivative (Savitzky–Golay filter with 21 smoothing points) in spectral bands of 3653–2775 and 1775–1188 cm^{-1}. Clear clustering of wood samples due to provenance was noticed. It is possible to quantify influence of specific wavenumbers (functional groups of wood polymers) by interpreting PCA loadings. Table 4 presents a summary of such analysis. Infrared spectroscopy, due to its operating principles, is only capable of detecting the presence of functional groups such as —OH, —CH or —CH_2. As can be seen, the lignin is most varying wood chemical component and predominantly affected the PCA model (gauiacyl rings at 1265 cm^{-1}, benzene rings at 1505 cm^{-1} and C=O vibrations at 1724 cm^{-1}). It has the

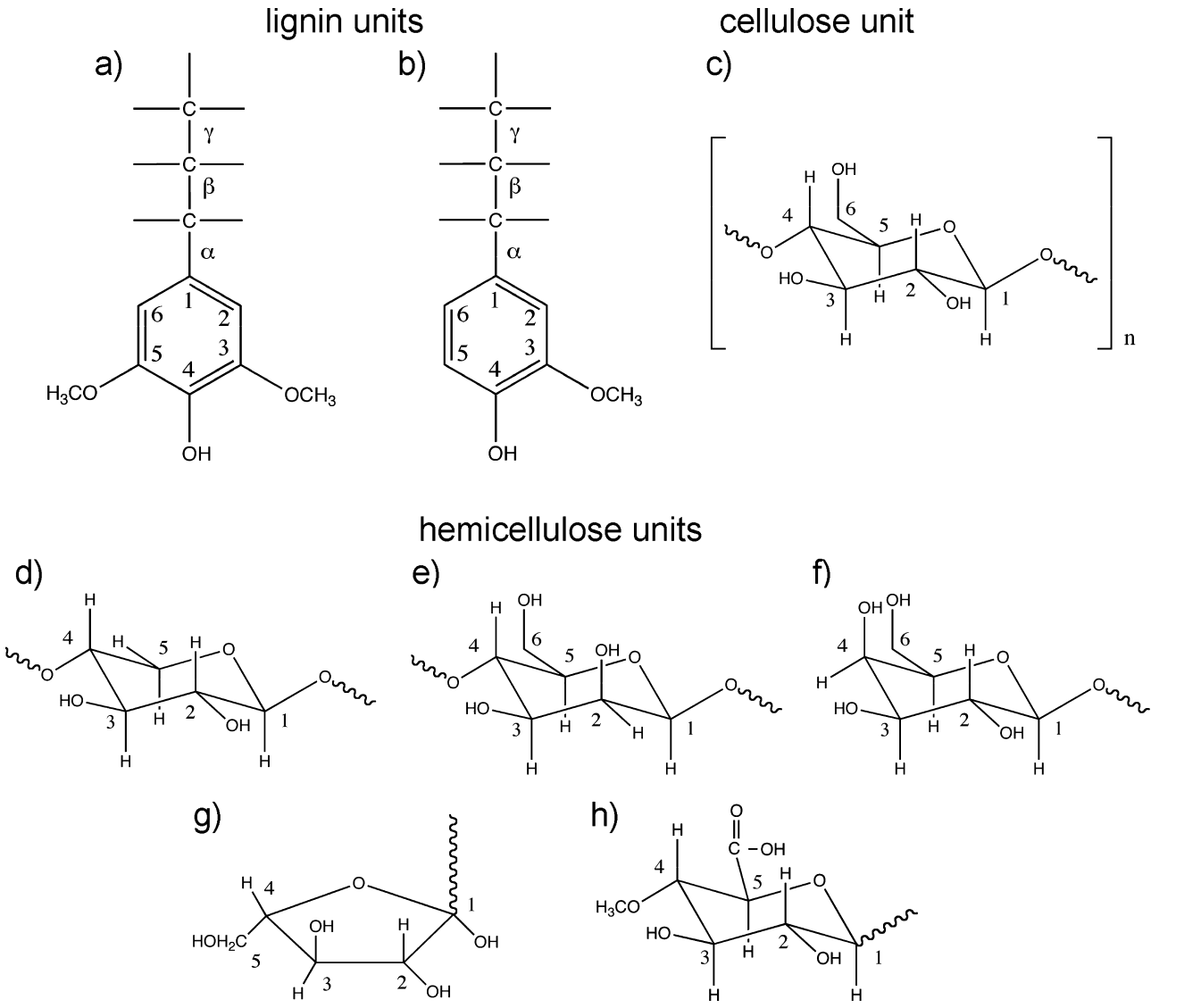

Fig. 2. Chemical structure of the wood components units in softwood; lignin: syringyl S (a) and guaiacyl G (b), cellulose: glucose (c), hemicelluloses: xylose (d), mannose (e), galactose (f), arabinose (g) methylglucuronic acid (h). *Note:* the numbering scheme corresponds to the resonance peaks summarized in Table 4.

Table 4
Interpretation of PCA loadings (L1–L3) of the model discriminating wood due to provenence and FT-IR spectra (L—lignin, H—hemicellulose, C—cellulose, W—water).

Nr.	Band assignment	Wavenumber (cm^{-1})	Wood component	L1	L2	L3
1	Syringil ring; C—O stretching of lignin and xylan	1226	L H	●	●	•
2	Guaiacyl ring	1265	L	●	●	●
3	C—H vibrations in cellulose; C—O in syringil derivatives	1319	C L	●	•	X
4	Vibration of O—H in lignin	1333	L	●	•	X
5	C—H deformation in cellulose and hemicelluloses	1363	C H	●	●	X
6	C—H bending vibrations in cellulose and hemicelluloses	1363	C H	●	●	X
7	C—H deformation in lignin and carbohydrates	1417	L C H	●	●	•
8	Aromatic skeletal vibrations combined with C—H in plane deformation	1417	L	●	●	•
9	Deformation of C—H in lignin and carbohydrates	1456	L C H	●	●	●
10	deformation of CH_3 and CH_2 of aromatic ring of lignin	1456	L	●	●	●
11	Benzene ring vibration of lignin	1505	L	●	●	•
12	Conjugated C—O	1587		●	●	●
13	Stretch of C=C of coniferyl alcohol + C=O of coniferyl aldehyde	1658		●	●	•
14	Unconjugated vibration of C=O of lignin and hemicelluloses	1724	L H	●	●	●
15	Stretching of C—H of lignin	2286	L	X	●	●
16	O—H vibration of water	3300	W	X	●	●

● Big influence ● medium influence • small influence X no influence.

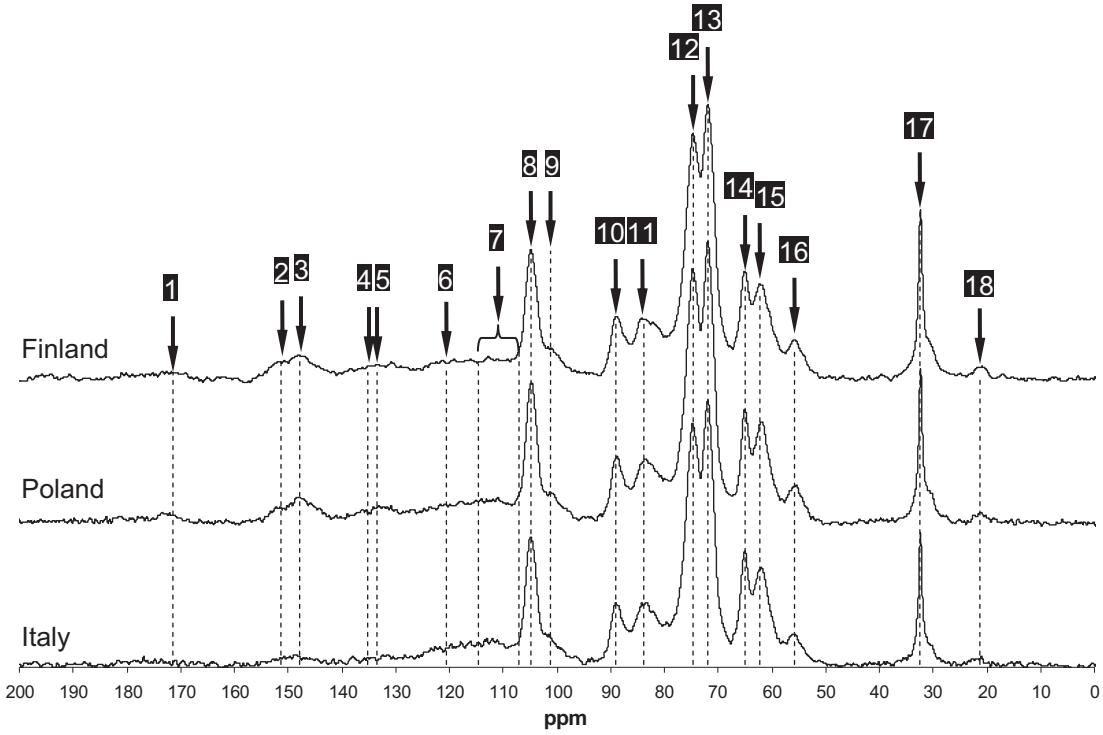

Fig. 3. NMR spectra of spruce woods differing in provenance and the peaks assignments. (17—HDPE reference).

highest influence on all loadings (L1, L2 and L3) highly differentiating wood samples investigated. On the other hand, spectral bands corresponding to cellulose and hemicelluloses are also contributing to the variance, even if with less significance.

FT-IR spectroscopy, ensures a good separation among wood samples, but cannot give an overall picture of the material composition. Therefore, solid state NMR was selected as an additional technique for providing supplementary/alternative set of information on the molecular structure at short and medium order. As already mentioned, a good fingerprint of wood samples can be obtained with ^{13}C CPMAS NMR measurements. Representative NMR spectra of wood from Finland, Poland and Italy are shown in Fig. 3. The spectra present the typical resonances of wood components that produce highly overlapped signals. Two key regions; from 160 to 110 ppm and from 110 to 15 ppm, can be distinguished in the NMR spectra, according to Bardet et al. (2009). The first is characterized by broad and low intensity resonances typical of the aromatic structures in lignin. The second region includes sharp intense peaks due to carbohydrate polymers (cellulose and hemicellulose) that are highly overlapping each other due to their chemical similarity.

Table 5 shows the resonance assignments (indicated by the numbering scheme in Fig. 3 and corresponding to the carbon atoms labeled in Fig. 2). It should be mentioned that ^{13}C CPMAS NMR spectroscopy allows for the distinction of chemically equivalent carbons in different chain packings or conformations, as it is in the

Table 5
^{13}C CPMAS resonance assignments of wood based on Bardet et al. (2009), Hult, Larsson and Iversen (2000), Xue, Wena, Xu and Sun (2012). In bold e = etherified in arylglycerol β-aryl ethers, ne = non-etherified.

Signal number*	Chemical shift (ppm)	Polymer main assignments	Carbon atom**
1	172.0	Carbohydrate	—C̲OO—R, CH$_3$—C̲OO—
2	152.6	Lignin	S3, S5 **e** in β-*O*-4
3	147.0	Lignin	S3, S5 **ne** in β-*O*-4, G3 **ne**, G4 **e**
4	136.0	Lignin	S1, S4 **e** in β-*O*-4; G1 **e** in β-*O*-4, S1 in β–β
5	134.3	Lignin	S1, S4 **ne** in β-*O*-4, G1 **ne** in β-*O*-4, S5, G5 in 5–5 units
6	121.0	Lignin	G6 **e** and **ne**
7	114–106	Lignin	G5 **e** and **ne**, G2, S2, S6
8	104.8	Carbohydrates	C1
9	101.9	Carbohydrates	C1 hemicellulose
10	88.7	Carbohydrates	C4 crystalline cellulose
11	83.8	Carbohydrates	C4 amorphous cellulose and hemicellulose, lignin Cβ in β-*O*-4, Cα in α-*O*-4
12	74.8	Carbohydrates	C2,3,5 Cellulose and hemicellulose; lignin Cα
13	72.2	Carbohydrates	C2,3,5 Cellulose and hemicellulose, Cα in β-*O*-4, Cγ in β–β
14	64.7	Carbohydrates	C6 cellulose and hemicellulose
15	61.6	Lignin	Cγ, Cγ in β-*O*-4, C6 cellulose and hemicellulose
16	55.7	Lignin	OCH$_3$
17	32.3	Polyethylene	—CH$_2$—
18	21.0	Carbohydrates	C̲H$_3$—COO—

The underline specifies the carbon atom associated to the chemical shift.
* Reported in Fig. 3.
** According to labeling of Fig. 2.

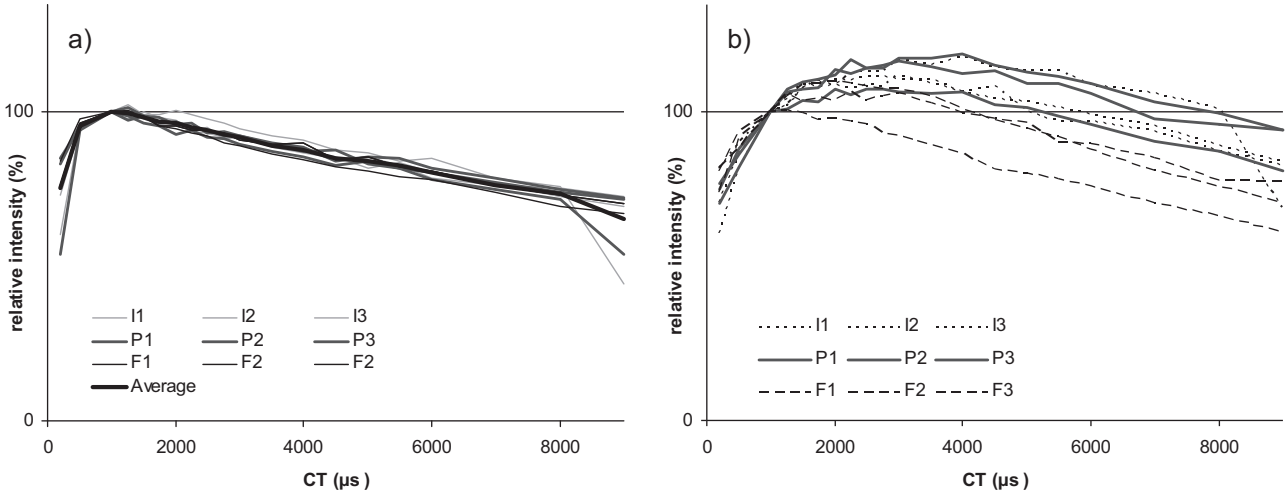

Fig. 4. Normalized peak intensity vs ct of HDPE signal 17 (a) and wood signal 8 (b).

case of amorphous and crystalline cellulose. The most intense peaks 12 and 13 are due to C-2, C-3 and C-5 carbons in carbohydrates. The two peaks 10 and 11 are assigned to C-4, in crystalline and amorphous (or less ordered surface) cellulose, respectively. Peak 15 is related to C-6 in cellulose and Cγ in lignin. Peak 8 represents cellulose's C-1 with a high-field shoulder 9 attributed to hemicellulose (102 ppm). Only two signals can be undoubtedly attributed to hemicellulose: the methyl carbon peak 18 and the carboxylic carbon signal 1, although these are of rather weak intensity. The three aromatic units constituting the lignin lattice are recognized from three groups of signals in the range 160–105 ppm. Finally, the small peak 16 is assigned to the lignin methoxyl group.

The three representative NMR spectra of Fig. 3 suggest that all the provenances (P, F and I) produce similar signals and only minor intensity differences can be noticed without a quantitative analysis,

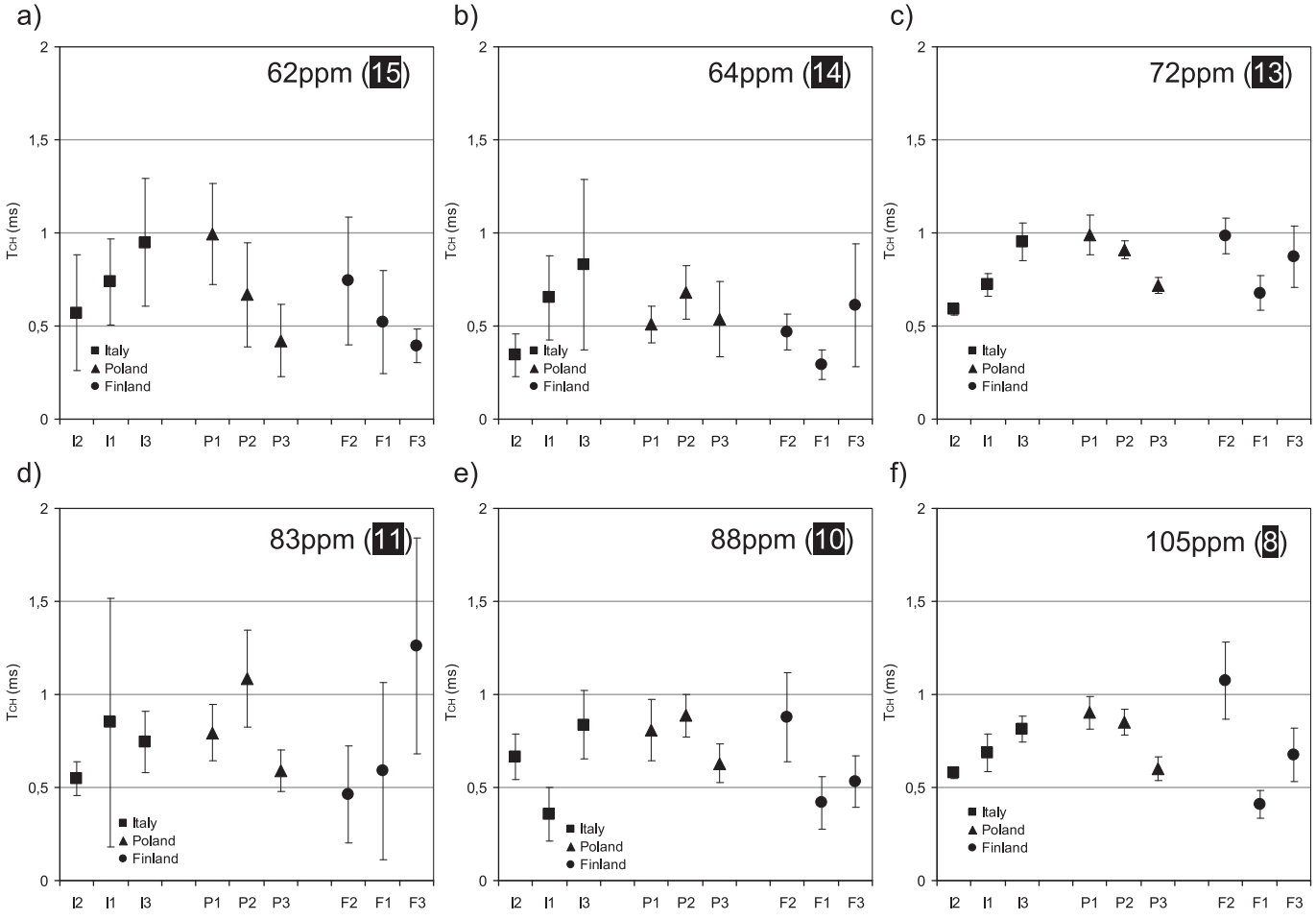

Fig. 5. T_{CH} values obtained from the fitting of VCT curves of selected ^{13}C signals with Eq. (1).

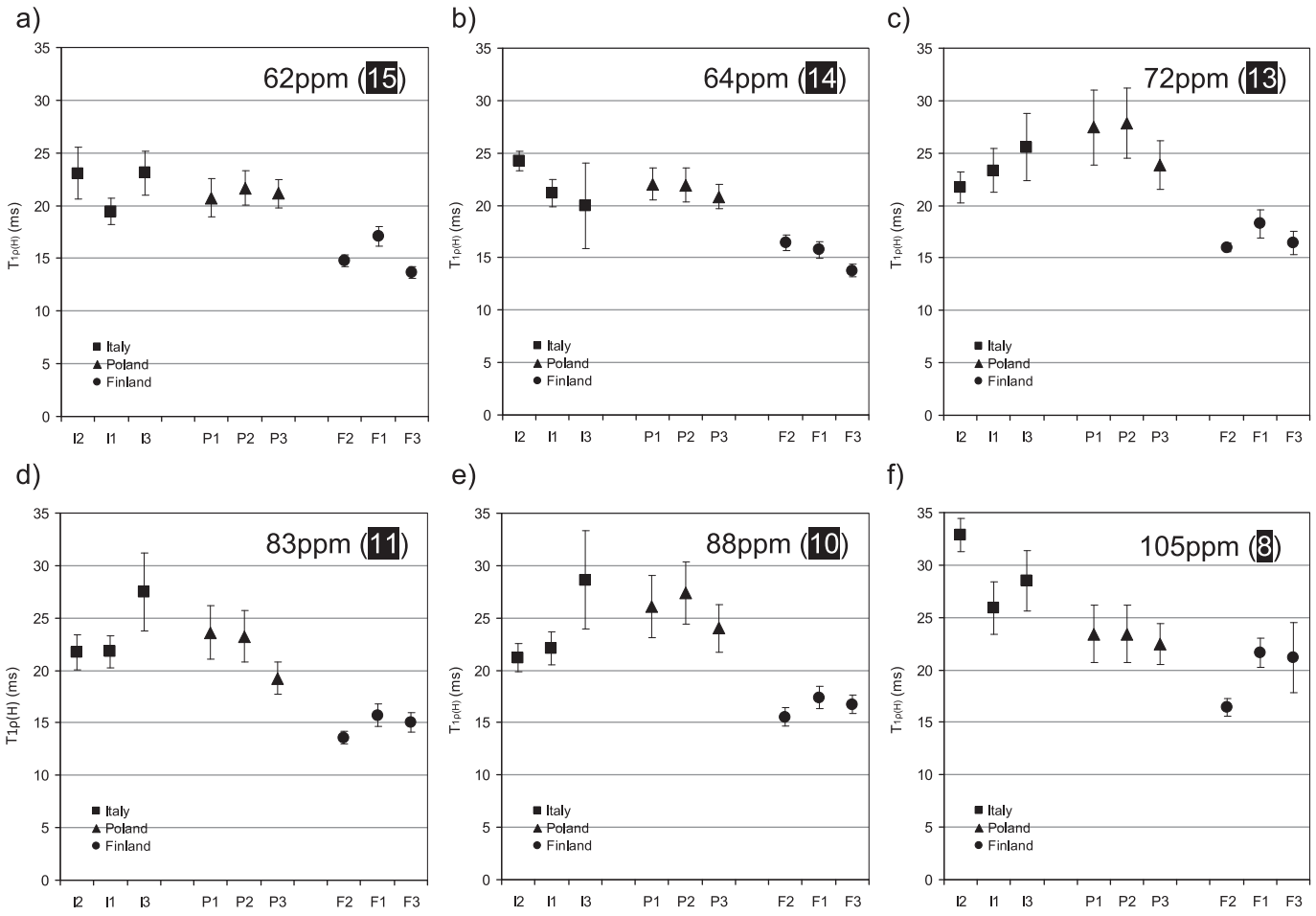

Fig. 6. $T_{1\rho(H)}$ values obtained from fitting VCT curves of selected ^{13}C signals with Eq. (1).

for example: lignin's peaks (3, 6, 7, 15) and carbohydrates' signals (1, 14, 18).

Chemically equivalent carbons produce the same response to cross-polarization and the resulting peak areas are comparable. For that reason, an internal standard has been used allowing for both quantitative spectra evaluation and probing the stability of the dynamic NMR measurements. The polyethylene (HDPE) standard produces a single sharp peak at 32 ppm corresponding to the methylene carbon of the polymer backbone (16 in Fig. 3). It was proved in the preliminary tests with the wood samples used that the HDPE peak does not overlap with wood signals and, in consequence, its intensity may be used for signal normalization and the estimation of the measurement error. HDPE was selected because the analyzed materials do not show any peaks in the 25–45 ppm range. Although this is the region of terpenic signals, these were not visible in measured samples. As a matter of fact, terpenes contribute to wood for less than 1.5%w (the average amount of extractives in our samples as shown in Table 2) and can be easily released during wood exposition to air, conditioning, storage and/or sample manipulation.

Additional NMR analyses were done because the straightforward comparison of raw NMR spectra was not sufficient for undoubtable discrimination of the wood provenances. Therefore, Dynamic NMR measurements were performed in order to provide supplementary information on the polymeric interconnections testing wider material domains. A series of CPMAS spectra were collected for each sample varying the contact time (ct) between 0.2 and 9.0 ms. The calculated signal intensity vs. contact time was compared after the normalization of the peak height. To neglect differences due to variations in sample weights, the intensity values of the selected peak y_n were extracted from the spectra and normalized with respect to the corresponding peak intensity at $ct = 1$ ms (y_1) according to the following equation:

$$y'_n = \frac{y_n}{y_1} \times 100 \quad (2)$$

The resulting y'_n values were plotted against the contact time. The HDPE signal (17) was used to ensure the reproducibility of the measurement procedure. The obtained results are presented in Fig. 4a. The HDPE VCT curves show similar profiles independently of the wood sample. The reproducibility of the measurements was good except for the shortest and the longest contact times, due to the relatively low signal intensity. Thus for the peak 17, the calculated measurement percentage error was ±6%.

Since CP spectral intensity is a measure of the efficiency of magnetization transfer from ^1H to ^{13}C by the dipolar coupling, the CP time constant (T_{CH}) can give a quantitative description of the cross-polarization and relaxation behavior (Abelmann, Totsche, Knicker, & Kogel-Knabner, 2004; Cheng, Wartelle, Klasson, & Edwards, 2010). The less mobile carbon groups exhibit both fast cross-polarization rate, i.e. short T_{CH}, because the cross-polarization is most efficient for the static ^1H—^{13}C dipolar interactions, and long $T_{1\rho(H)}$ values. As mobility increases (i.e., with increasing

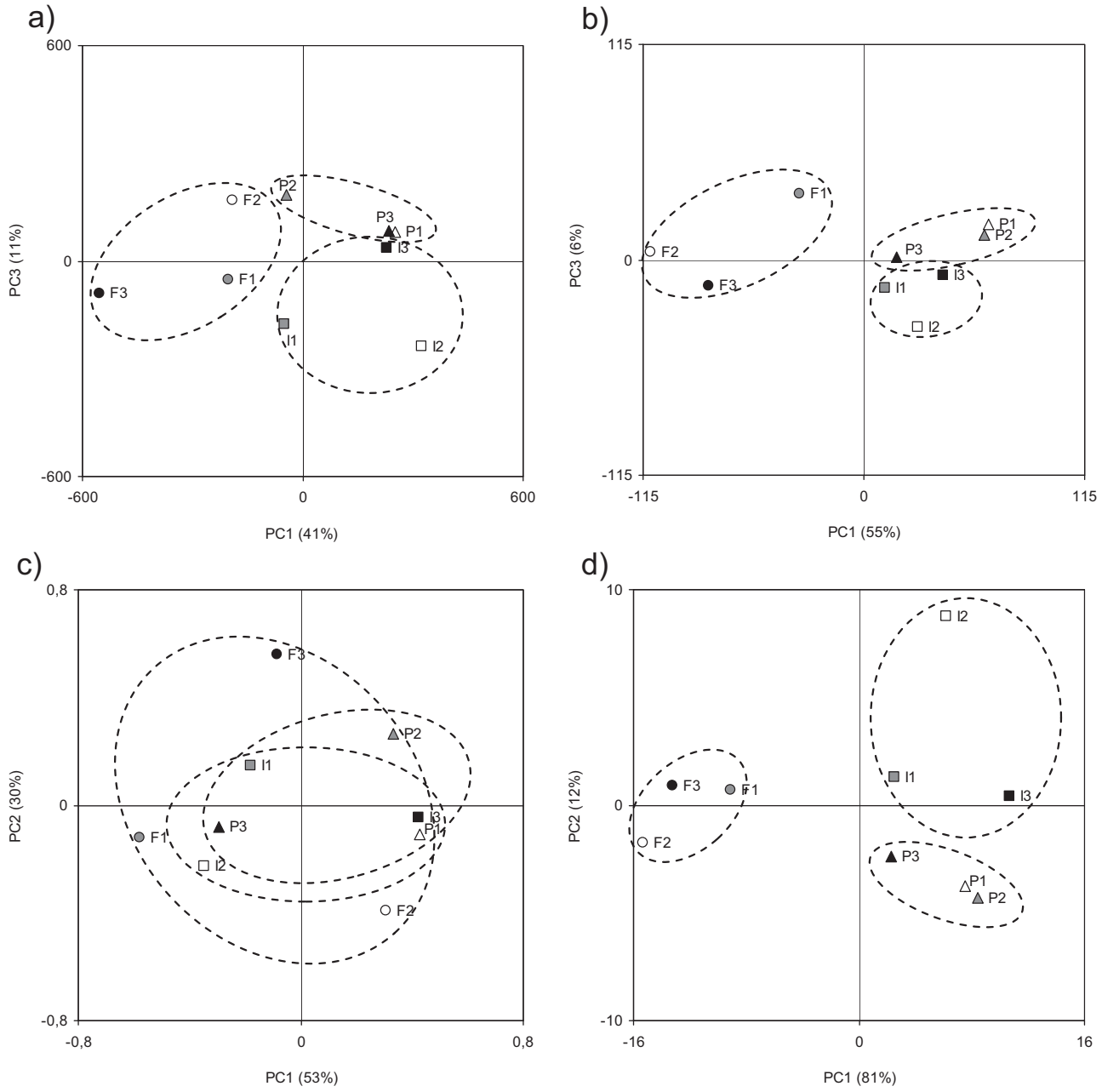

Fig. 7. Principal components analysis of; all NMR spectra (a), dataset of all the VCT curves of selected peaks (b) and T_{CH} (c) and $T_{1\rho(H)}$ (d) computed from VCT curves.

amorphous or homogeneous character of sample series) T_{CH} increases and $T_{1\rho(H)}$ decreases. It has been demonstrated that the measure of $T_{1\rho(H)}$ relaxation time can be used to estimate the domain size in polymers (Conte, Spaccini, & Piccolo, 2006). Diffusion of ^{1}H magnetization within a hybrid system tends to average the ^{1}H relaxation time thus leading to an averaging effect on the $T_{1\rho(H)}$ of the different components. In a homogeneous system, a single spin–lattice relaxation time is usually observed. For a heterogeneous system, more than one $T_{1\rho(H)}$ value are often found, because there is insufficient time for spin diffusion to equilibrate the magnetization in different phases (Kao, Chao, & Chang, 2006). Through measures of contact time variation, mobility and interactions of polymers can be studied (Bardet et al., 2009; Okushita et al., 2012). Actually, similar relaxation times of polymeric species inside the same matrix correspond to chemical interactions between chains (Liitia, Maunu, & Hortling, 2000, 2001; Bardet et al., 2009).

HDPE is a homogeneous polymer, and therefore, the magnetization behavior follows the single exponential law (Eq. (1)). The calculated values of both time constants (T_{CH} = 0.17 μs and $T_{1\rho(H)}$ = 21.1 μs) were in agreement with the results reported for HDPE measurements in similar conditions (Nogueira, Tavares, & Nogueira, 2004). It was possible to conclude therefore that polyethylene was a suitable reference and that all the experimental results from tests are comparable.

The wood spectra display intense sharp peaks together with weak and broad resonances. In order to keep the confidence level of 6%, the exponential trend of intensity vs. contact time was studied only for some selected peaks. These are the sharpest and fall in the range between 110 and 60 ppm. Accordingly, seven peaks were chosen: (8) C-1 from cellulose, (10), C-4 from crystalline cellulose, (11), C-4 from amorphous cellulose and Cβ from lignin, (12), C2,3,5 from cellulose and Cα from lignin, (13), C2,3,5 from cellulose, (14),

CH_2OH C-6, and (15), Cγ from lignin. Examples of the VCT curves related to peak 8 at 105 ppm are presented in Fig. 4b. The above peak selection includes mainly the cellulose peaks, but the overall signal overlapping ensures also the contribution of other woody polymers. Assuming that all the carbons are in similar motional domains, the rising part of the exponential curve is dominated by the static dipolar interaction between carbon atom and nearest neighbor protons ($^{13}C—^{1}H$ distance) described by the T_{CH} relaxation time. The T_{CH} values for the evaluated signals are shown in Fig. 5. It is clear that variations of T_{CH} do not display particular trends due to sample provenance and any differences among the samples are not systematic.

The obtained average T_{CH} values, around 0.7 ms, can be considered as the result of the presence of both rapidly and slowly cross-polarizing components, with a predominance of the latter. In literature, it was reported that the determination of T_{CH} is inherently difficult because, in principle, there are as many T_{CH} values as there are chemical environments. In the studied case, the values were closer to those typical of aromatics, in particular for samples from Italy and Poland (Conte et al., 2006). This could also be explained with the presence of small proton-rich hydrophobic domains or short polymeric chains randomly distributed within the wood cell walls.

In case of rigid and heterogeneous materials, such as wood, Eq. (1) is a good model because the assumption $T_{CH} \ll T_{1\rho(H)}$ is satisfied. The effect of relaxation due to spin diffusion is therefore commonly investigated (Smernik, Baldock, & Oades, 2002; Nogueira et al., 2004). The $M(t)$ curve fitting was performed by means of only one exponential factor, due to the high complexity of the system. Additionally, consideration of multiple exponential fitting factors did not significantly improve the result. The average extrapolated parameters $T_{1\rho(H)}$ for each peak are presented in Fig. 6. It should be noticed that for most peaks the $T_{1\rho(H)}$ values can be clustered according to the geographical provenance of wood. In particular, samples from Finland, show uniform values that are clearly lower than those of samples from other series. High values of $T_{1\rho(H)}$ are related to slow motion and minimized variations among $T_{1\rho(H)}$ values for different peaks suggest an intimate connection among the structural components of wood. Quite homogeneous values are found for the samples from Poland, with the exception of peaks 11 and 13. The series of Italian woods posses more scattered values, especially for peaks 8, 10, and 11. In general, samples from Italy and Poland show rather analogous results with the exception of the resonance 8. The C-1 $T_{1\rho(H)}$ (peak 8) produces the highest discrimination among samples and suggests that mobility increases according to Italy < Poland < Finland trend.

It is possible to notice some correlations among the physical features of wood (presented in Table 3) by considering the $T_{1\rho(H)}$ values as derived from the molecular organization of polymers. The $T_{1\rho(H)}$ trend of the peak 8 (cellulose C-1) highlights that samples with higher density display smaller relaxation times, suggesting a relationship between these two parameters ($r^2 = 0.92$). Similarly, the $T_{1\rho(H)}$ of peak 10 (crystalline cellulose) could be correlated with the quantity of latewood ($r^2 = 0.85$), i.e. samples with higher latewood ratio show shorter relaxation time. The peculiar characteristics of wood from Finland might be interpreted by distinct chemical and physical properties of trees growing in Scandinavia, i.e. the highest wood density, high ratio of late wood, and relatively high extractives content. All these are clearly related to the climatic conditions that shorten the growth periods and stimulate the development of efficient defence systems against local pathogens.

Multivariate analyses, similar to those performed on the FT-IR spectra were applied as well to NMR data. The results obtained are summarized in Fig. 7. The PCA discrimination of the NMR spectra (obtained with $ct = 1.0$ ms) did not provide sufficient differences for undoubtable discrimination of wood samples from different provenances. As shown in Fig. 7a, the values of the samples from Poland (P1 and P3) overlapped the values of samples from Italy (I3). Some improvement of the discrimination algorithm was achieved by computing the principal components from VCT curves of selected peaks (8, 10, 12, 13, 14, 15) and is presented in Fig. 7b. Component PC1 alone (explaining 55% of the variance) was sufficient for separation of Finnish samples from other provenances. On the other hand, the clear discrimination of Polish samples from Italian samples based on component PC3 was limited as both clusters were close to each other and even slightly overlapping.

A significant improvement of the origin determination capability of the software was achieved after performing PC analysis of the VCT experimental results, but only analyzing $T_{1\rho(H)}$ coefficients. Actually, it was impossible to create any reliable PCA model for discrimination of wood origin based only on the T_{CH} coefficients. Fig. 7c shows the overlapping of the clusters even if both principal components covered over 83% of the variance. This is in agreement with the previous considerations on T_{CH} presented in the NMR section. The PCA scores from analysis of the $T_{1\rho(H)}$ coefficients are shown in Fig. 7d. PC1 (explaining 81% of the variance within spectra) separates samples into two groups: Finland (with PC1 values of negative order) and Poland/Italy (with positive values of PC1). Moreover, PC2 (explaining 12% of the data variance) separates samples coming from Italy and those originating from Poland. The cluster distribution is slightly similar to that of Fig. 7b, but the most important difference is the higher spectral distance of Italian and Polish samples assuring an apparent differentiation of the wood provenance.

4. Conclusions

The work presented here was devoted to the development of a novel methodology for characterization and discrimination of a wood in regard to its origin on the basis of infrared and nuclear magnetic resonance spectra. The requirement was to use untreated solid wood samples to minimize any manipulation to the nanostructure of native wood. The results confirm that the chemical and physical properties of samples belonging to the same wood species (*P. abies* L. Karst.) differ due to the origin. Both FT-IR and dynamic NMR spectroscopies were able to discriminate correctly samples originating from three different provenances in Europe. The successful discrimination by means of infrared spectroscopy was mostly related to differences in the molecular configuration (functional groups) of lignin with some contribution of cellulose and hemicellulose. Although the number of analyzed samples in the present work cannot be considered statistically meaningful, the results clearly indicated that FTIR outcomes can be confirmed by means of solid state nuclear magnetic resonance. NMR also permits to highlight additional differences both in the connections among constitutional polymers and in the homogeneity of molecular domains within wood samples of different provenances.

The measurement reliability of the NMR experiment has been quantified by means of internal reference in form of HDPE strip rolled together with wooden sample. It was also possible to normalize the spectra according to the wood/HDPE mass ratio.

The most effective chemometric tool for discrimination of spectra due to provenance was principal components analysis. It provided reliable prediction models for infrared spectroscopy, but was also very useful for analysis of NMR spectra. In the second case the analysis of $T_{1\rho(H)}$ coefficients as computed from fitting the $M(t)$ curve was the most efficient. Further interpretation of $T_{1\rho(H)}$ suggests a higher polymer mobility and a higher homogeneity in wood from Finland. On the other hand, equally less homogeneity was noticed in wood samples from both Italy and Poland. Discrimination of provenance was achieved by means of $T_{1\rho(H)}$ PC analyses.

This was expected, and it followed both theoretical background and literature references.

In conclusion, it was possible to apply presented methodologies for the characterization of wood according to its origin by means of both infrared and nuclear magnetic resonance spectroscopies. Such methods might be very useful for both, research and understanding of wood microstructure and its variations induced by growth conditions.

Acknowledgments

Part of this work has been conducted within the framework of the project SWORFISH (team 2009 incoming (CALL 2) and Trentino—PCOFUND-GA-2008-226070) co-financed by Provincia Autonoma di Trento. John Downs, PhD, is greatly acknowledged for the English text revision.

References

Abelmann, K., Totsche, K. U., Knicker, H., & Kogel-Knabner, I. (2004). CP dynamics of heterogeneous organic material: Characterization of molecular domains in coal. *Solid State Nuclear Magnetic Resonance*, *25*, 252–266.

Aghemo, C., Albertino, A., & Gobetto, R. (2011). Isotopic Analysis and ^{1}H-NMR Spectroscopy for Traceability and Discrimination of Italian Wines. In J. P. Renou, G. A. Webb, & P. S. Belton (Eds.), *Magnetic resonance in food science: An exciting future* (pp. 30–35). Cambridge: RCS Publications.

Alesiani, M., Proietti, F., Capuani, S., Paci, M., Fioravanti, M., & Maraviglia, B. (2005). ^{13}C CPMAS NMR spectroscopy analysis of recent and archeological wood. *Applied Magnetic Resonance*, *29*, 177–184.

Andreassen, K., Solberg, S., Tveito, O. E., & Lystad, S. L. (2006). Regional differences in climatic responses of Norway spruce (*Picea abies* L. Karst) growth in Norway. *Forest Ecology & Management*, *222*, 211–221.

Bardet, M., Foray, M. F., & Tran, Q. K. (2002). High-resolution solid-state CPMAS NMR study of archaeological woods. *Analytical Chemistry*, *74*, 4386–4390.

Bardet, M., Foray, M. F., Maron, S., Goncalves, P., & Tran, Q. K. (2004). Characterization of wood components of Portuguese medieval dugout canoes with high-resolution solid-state NMR. *Carbohydrate Polymers*, *57*, 419–424.

Bardet, M., Gerbaud, G., Giffard, M., Doan, C., Hediger, S., & Le Pape, L. (2009). ^{13}C high resolution solid-state NMR for structural elucidation of archaeological woods. *Progress in Nuclear Magnetic Resonance Spectroscopy*, *55*, 199–214.

Browning, B. L. (1967). *The chemistry of wood*. New York, NY: Interscience (Wiley).

Burns, D. A., & Ciurczak, E. W. (2008). *Handbook of near-infrared analysis*. Boca Raton, FL: CRC Press (Taylor & Francis Group).

Capanema, E. A., Balakshin, M. Y., & Kadla, J. F. (2004). A comprehensive approach for quantitative lignin characterization by NMR spectroscopy. *Journal of Agricultural and Food Chemistry*, *52*, 1850–1860.

Cheng, H. N., Wartelle, L. H., Klasson, K. T., & Edwards, J. C. (2010). Solid-state NMR and ESR studies of activated carbons produced from pecan shells. *Carbon*, *48*, 2455–2469.

Conte, P., Spaccini, R., & Piccolo, A. (2006). Advanced CPMAS-^{13}C NMR techniques for molecular characterization of size-separated fractions from a soil humic acid. *Analytical and Bioanalytical Chemistry*, *386*, 382–390.

Crestini, C., El Hadidi, N., & Palleschi, G. (2009). Characterization of archaeological wood: A case study on the deterioration of a coffin. *Microchemical Journal*, *92*(2), 150–154.

Darwin, C. (1868). . *The variation of animals and plants under domestication* (vol. 1) London: Murray.

Delmotte, L., Ganne-Chédeville, C., Leban, J. M., Pizzi, A., & Pichelin, F. (2008). CP MAS ^{13}C NMR and FTIR investigation of the degradation reactions of polymer constituents in wood welding. *Polymer Degradation and Stability*, *93*, 406–412.

Dykstra, D. P., Kuru, G., Taylor, R., Nussbaum, R., Magrath, W. B., & Story, J. (2002). Technologies for wood tracking—verifying and monitoring the chain of custody and legal compliance in the timber industry. Environment and social development East Asia and Pacific region discussion paper. In *World Bank—WWF Alliance report*. World Bank., http://www.proforest.net/publication (accessed 30.10.2013).

Fengel, D., & Wegener, G. (1989). *Wood: Chemistry, ultrastructure, reactions*. Berlin: Walter de Gruyter.

Franceschini, T., Bontemps, J. D., Gelhaye, P., Rittie, D., Herve, J. C., Gegout, J. C., et al. (2010). Decreasing trend and fluctuations in the mean ring density of Norway spruce through the twentieth century. *Annals of Forest Science*, *67*, 816.

Gil, A. M., & Neto, P. C. (1999). Solid state NMR studies of wood and other lignocellulosic materials. *Annual Reports on NMR Spectroscopy*, *37*, 75–117.

Hult, E. L., Larsson, P. T., & Iversen, T. (2000). A comparative CP/MAS 13C-NMR study of cellulose structure in spruce wood and kraft pulp. *Cellulose*, *7*, 35–55.

Kao, H. M., Chao, S. W., & Chang, P. C. (2006). Multinuclear solid-state NMR, self-diffusion coefficients, differential scanning calorimetry, and ionic conductivity of solid organic–inorganic hybrid electrolytes based on PPG–PEG–PPG, diamine, siloxane, and lithium perchlorate. *Macromolecules*, *39*, 1029–1040.

Kolodziejski, W., & Klinowski, J. (2002). Kinetics of cross-polarization in solid state NMR: A guide for chemists. *Chemical Reviews*, *102*, 613–628.

Krzysik, F. (1978). *Nauka o drewnie*. Warszawa: PWN (in Polish).

Larsson, P. T., Hult, E. L., Wickholm, K., Pettersson, E., & Iversen, T. (1999). CP/MAS ^{13}C-NMR spectroscopy applied to structure and interaction studies on cellulose I. *Solid State Nuclear Magnetic Resonance*, *15*, 31–40.

Liitiä, T., Maunu, S. L., & Hortling, B. (2000). Solid state NMR studies on cellulose crystallinity in fines and bulk fibers separated from refined kraft pulp. *Holzforschung*, *54*, 618–624.

Liitiä, T., Maunu, S. L., & Hortling, B. (2001). Solid state NMR studies on inhomogeneous structure of fiber wall in kraft pulp. *Holzforschung*, *55*, 503–510.

Malkavaara, P., Alén, R., & Kolehmainen, E. (2000). Chemometrics: An important tool for the modern chemist, an example from wood-processing chemistry. *Journal of Chemical Information and Computer Sciences*, *40*, 438–441.

Manetti, M. C., & Cutini, A. (2006). Tree-ring growth of silver fir (*Abies alba* Mill.) in two stands under different silvicultural systems in central Italy. *Dendrochronologia*, *23*, 145–150.

Maunu, S. L. (2002). NMR studies of wood and wood products. *Progress in Nuclear Magnetic Resonance Spectroscopy*, *40*, 151–174.

Mansfield, S. D., & Meder, R. (2003). Cellulose hydrolysis—The role of monocomponent [664] cellulases in crystalline cellulose degradation. *Cellulose*, *10*, 159–169.

Mazzei, P., & Piccolo, A. (2012). ^{1}H HRMAS-NMR metabolomic to assess quality and traceability of mozzarella cheese from Campania buffalo milk. *Food Chemistry*, *132*, 1620–1627.

Mburu, F., Dumarcay, S., Huber, F., Petrissans, M., & Gerardin, P. (2007). Evaluation of thermally modified *Grevillea robusta* heartwood as an alternative to shortage of wood resource in Kenya: Characterisation of physicochemical properties and improvement of bio-resistance. *Bioresource Technology*, *98*, 3478–3486.

Miina, J. (2000). Dependence of tree-ring, earlywood and latewood indices of Scots pine and Norway spruce on climatic factors in eastern Finland. *Ecological Modelling*, *132*, 259–273.

Miranda, I., & Pereira, H. (2002). Variation of pulpwood quality with provenances and site in *Eucalyptus globulus*. *Annals of Forest Science*, *59*, 283–291.

Newman, R. H. (1999). Estimation of the lateral dimensions of cellulose crystallites using ^{13}C NMR signal strengths. *Solid State Nuclear Magnetic Resonance*, *15*, 1–29.

Nielsen, L. R., & Kjær, E. D. (2008). *Tracing timber from forest to consumer with DNA markers*. Danish Ministry of the Environment, Forest and Nature Agency., ISBN 978-87-7279-815-8, http://curis.ku.dk/ws/files/8102944/TracingTimber.pdf (accessed 30.10.2013).

Nimz, H. H., Robert, D., Faix, O., & Nemr, M. (1981). Carbon-13 NMR spectra of lignins: Structural di3erences between lignins of hardwoods, softwoods, grasses and compression wood. *Holzforschung*, *35*, 16–26.

Nogueira, R. F., Tavares, M. I. B., & Nogueira, J. S. (2004). ^{13}C NMR molecular dynamic investigation of tropical wood Angelin Pedra (*Hymenolobium paetrum*). *Materials Sciences and Applications*, *2*, 453–457.

Okushita, K., Komatsu, T., Chikayama, E., & Kikuchi, J. (2012). Statistical approach for solid-state NMR spectra of cellulose derived from a series of variable parameters. *Polymer Journal*, *44*, 895–900.

Park, Y. I., & Spicker, H. (2005). Variation in the tree-ring structure of Norway spruce (*Picea abies*) under contrasting climates. *Dendrochronologia*, *23*, 93–104.

Popescu, C. M., Larsson, P. T., & Vasile, C. (2011). Carbon-13 CP/MAS solid state NMR and X-ray diffraction spectroscopy studies on lime wood decayed by *Chaetomium globosum*. *Carbohydrate Polymers*, *83*(2), 808–812.

Preston, C. M., Trofymow, J. A., Niu, J., & Fyfe, C. A. (1998). ^{13}C CPMAS-NMR spectroscopy and chemical analysis of coarse woody debris in coastal forests of Vancouver Island. *Forest Ecology and Management*, *111*, 51–68.

Rana, R., Müller, G., Naumann, A., & Polle, A. (2008). FTIR spectroscopy in combination with principal component analysis or cluster analysis as a tool to distinguish beech (*Fagus sylvatica* L.) trees grown at different sites. *Holzforschung*, *62*(5), 530–538.

Ritota, M., Casciani, L., Han, B. Z., Cozzolino, S., Leita, L., Sequi, P., et al. (2012). Traceability of Italian garlic (*Allium sativum* L.) by means of HRMAS-NMR spectroscopy and multivariate data analysis. *Food Chemistry*, *135*(2), 684–693.

Ritota, M., Casciani, L., Failla, S., & Valentini, M. (2012). HRMAS-NMR spectroscopy and multivariate analysis meat characterization. *Meat Science*, *92*(4), 754–761.

Sacchi, R., & Paolillo, L. (2007). NMR for food quality and traceability. In L. M. L. Nollet, & F. Toldrá (Eds.), *Advances in food diagnostics* (pp. 101–117). Ames, IA: Blackwell Publishing.

Sandak, A., Sandak, J., & Negri, M. (2010). Potential of mid and near infrared spectroscopy for geographical origin recognition of forest based biomasses. In *Proceedings of III International Symposium on Energy from Biomass and Waste* Venice, Italy, CISA Publisher.

Sandak, A., Sandak, J., & Negri, M. (2011). Relationship between near-infrared (NIR) spectra and the geographical provenance of timber. *Wood Science and Technology*, *45*(1), 35–48.

Sandak, J., Sandak, A., Cantini, C., & Autino, A. (2014). Differences in wood properties of Picea abies L. Karst. in relation to site of provenance and population genetics. *Holzforshung*, http://dx.doi.org/10.1515/hf-2014-0061, in press

Sivonen, H., Maunu, S. L., Sundholm, F., Jamsa, S., & Viitaniemi, P. (2002). Magnetic resonance studies of thermally modified wood. *Holzforschung*, *56*, 648–654.

Sjöström, E. (1981). *Wood chemistry, fundamentals and applications*. San Diego, CA: Academic Press, Inc.

Skrøppa, T., Hylen, G., & Dietrichson, J. (1999). Relationship between wood density components and juvenile height growth and growth rhythm trials for Norway spruce provenances and families. *Silvae Genetica*, *48*(5), 235–239.

Smernik, R. J., Baldock, J. A., & Oades, J. M. (2002). Impact of remote protonation on ^{13}C CPMAS NMR quantitation of charred and uncharred wood. *Solid State Nuclear Magnetic Resonance*, *22*, 71–82.

Smith, R. H., Peloquin, R. L., & Passoff, P. C. (1969). *Local and regional variation in the monoterpenes of ponderosa pine wood oleoresin*. Oxford: U.S.D.A forest Serv Res paper PSW-56., 10pp.

Spicker, H. (2000). Growth of Norway spruce (*Picea abies* [L.] Karst.) under changing environmental conditions in Europe. *EFI Proceedings*, *33*, 11–26.

Tahar, D., Tayeb, B., & Chaabane, C. (2007). Essential oil composition of *Pinus halepensis* Mill. from three different regions in Algeria. *Journal of Essential Oil Research*, *19*, 40–43.

Tappi Standard. (2006). *T 222 om-06. Acid insoluble lignin in wood and pulp*. Tappi Standard.

Tappi Standard. (2007a). *T 204 cm-07. Solvent extractives of wood and pulp*. Tappi Standard.

Tappi Standard. (2007b). *T 212 om-07. One percent sodium hydroxide solubility of wood and pulp*. Tappi Standard.

Tappi Standard. (2007c). *T 211 om-07. Ash in wood, pulp, paper and paperboard: Combustion at 525 °C*. Tappi Standard.

Tappi Standard. (2008). *T 207 cm-08. Water solubility of wood and pulp*. Tappi Standard.

Viel, S., Capitani, D., Proietti, N., Ziarelli, F., & Segre, A. L. (2004). NMR spectroscopy applied to the cultural heritage: A preliminary study on ancient wood characterization. *Applied Physics A: Materials Science & Processing*, *79*, 357–361.

Xue, B., Wena, J., Xu, F., & Sun, R. (2012). Structural characterization of hemicelluloses fractionated by graded ethanol precipitation from Pinus yunnanensis. *Carbohydrate Research*, *352*, 159–165.